Waste and Biomass Valorization (2024) 15:1901–1915
https://doi.org/10.1007/s12649-023-02386-z

ORIGINAL PAPER

In-vitro Evaluation of *Talaromyces islandicus* Mediated Zinc Oxide Nanoparticles for Antibacterial, Anti-inflammatory, Bio-pesticidal and Seed Growth Promoting Activities

M. K. Sangeeta[1] · Tejashree[1] · Vidyasagar M. Gunagambhire[1] · Meghashyama Prabhakara Bhat[2] · Shashiraj Kariyellappa Nagaraja[2] · Pooja V. Gunagambhire[2] · Raju Suresh Kumar[3] · Sakkarapalayam M. Mahalingam[4]

Received: 26 September 2023 / Accepted: 7 December 2023 / Published online: 22 January 2024

Abstract

Nanoparticles (NPs) are regarded as the most significant innovation of the twentieth century to produce biological materials at the nanoscale level, with numerous applications for human welfare. In this study, *Talaromyces* extract-coated zinc oxide nanoparticles (ZnONPs) were synthesised, and their toxicity against human pathogenic bacteria via antibacterial and anti-inflammatory activity was investigated. In the meantime, the pesticidal efficacy against the green cloverworm (*Hypena scabra*) was assessed. Spectroscopy techniques were utilized to characterise ZnONPs. The UV spectrum peak indicated nanoparticle formation at 298 nm, and X-ray diffraction (XRD) analysis showed that nanoparticles were 22–34 nm in size and crystalline. The octagonal to spherical shape of NPs was determined using microscopy techniques such as SEM and AFM. EDX analysis confirmed the presence of elemental silver. Antimicrobial activity as compared to streptomycin, zinc oxide nanoparticles have demonstrated noteworthy efficacy against both *S. aureus* and *S. epidermis*, exhibiting inhibition zones measuring 10.33 ± 0.33 and 13 ± 0.33, respectively. Anti-inflammatory responses of nanoparticles evaluated using the human red blood cells (HRBC) membrane stabilisation method, egg albumin assay, and protein denaturation assay showed dose-dependent activity. The HRBC membrane stabilisation assay revealed 86–25% haemolysis rates for ZnONPs compared to 61–8% for standard aspirin at 100 and 500 µg/mL, respectively. Albumin denaturation assay of ZnONPs (100 µg/mL) demonstrated 37.89% inhibition compared to 61.96% inhibition by standard aspirin (100 µg/mL), whereas protein denaturation assay demonstrated ZnONPs 45.69% inhibition and std aspirin 60.67% inhibition, respectively. Evaluation of the pesticidal potential of ZnONPs against the green cloverworms revealed mortality rates of 28.57% at 24 h, 66.66% at 48 h and 83.33% at 72 h, respectively, having no detrimental effects on seed germination. According to our knowledge, this work is the first to document the mycosynthesis of zinc oxide nanoparticles (ZnONPs) using *Talaromyces islandicus*. This finding can potentially facilitate the synthesis of novel and economically viable nano-drugs through a microbial-based synthesis approach.

Graphical Abstract

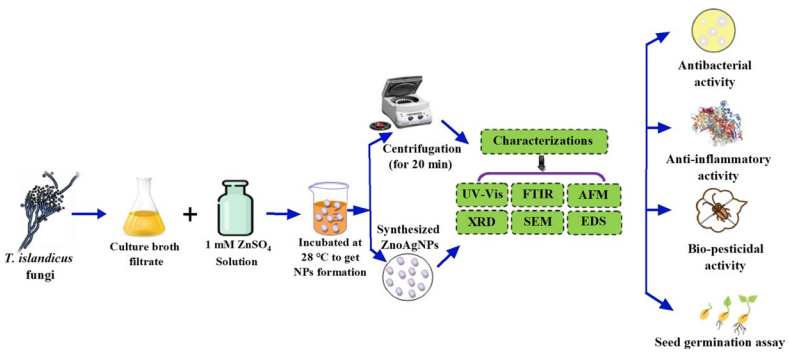

Extended author information available on the last page of the article

Keywords *Talaromyces islandicus* · ZnONPs · Anti-bacterial · Anti-inflammatory · Pesticidal activity · Seed growth promotion

Statement of Novelty

- The ZnONPs have most investigated inorganic nanoparticles and excellent choice in biological applications due to its low toxicity and biocompatibility.
- Biogenic synthesis of metal NPs from fungi are comparatively more resourceful than other natural sources.
- Interestingly, the ZnONPs showed significant zone of inhibition (ZOI) against Gram-positive bacteria as compared to the standard.
- To alleviate side effects of non-steroidal anti-inflammatory drug, it's important to find natural resource with no toxicity is recommended against inflammation.
- The indiscriminate use of chemical pesticides causing adverse effects on environment and as well human health, thus the production of nano-pesticides are functional aspects in agricultural sector.

Introduction

Nanostructures are ideal carriers of drugs in pharmaceutical science. With the advancement of nanotechnology research, novel findings are generated continuously, which can be utilized directly or indirectly in human welfare. Poorly soluble and permeable drugs cannot act efficiently at targeted sites. In such cases, nanocrystals or reducing the size of drugs at the nano level is the best way to increase the solubility and permeability of the drugs at the target site, resulting in a fast beginning of action [1]. Nanoparticles with unique characteristics like conductivity, catalysis, antimicrobial, anti-inflammatory, biopesticidal, and anticancer potential have inspired researchers to unfold their hidden potential in various scientific fields [2]. Employing microbes in producing nanoparticles with biological importance is easy and cost-effective. Because of its large size and more enzyme-producing ability, fungi are suitable for nanoparticle production. Fungi usually produce nanoparticles of uniform size in a dispersed phase with distinct dimensions [3]. Among the nanoparticles, the biosynthesis of ZnONPs has been appealing because of its extensive antimicrobial activity against pathogenic microbes [4–6]. The body's metabolic processes, DNA and protein synthesis, cell signaling, and cell division benefit from zinc, an essential ion. Additionally, ZnONPs have received the GRAS (generally recognized as safe) designation by the Food and Drug Administration (FDA) of the United States of America [7]. Zinc is part of numerous catalytic enzymes and is involved in insulin regulation. Hence, in this paper, an attempt is made to synthesize ZnONPs from fungi.

Zinc nanoparticles have been synthesized through various techniques such as hydro-thermal, sol–gel, chemical vapour deposition, direct deposition, and spray pyrolysis. Some of these methods require particular experimental conditions that are tedious or needs advanced equipment. However, these methods are not eco-friendly as they require high temperature, pressure, toxic chemicals during the synthesis process [8]. Microorganisms secrete numerous extracellular secondary metabolites and bio-molecules in culture broth. Those biomolecules when react with the metal ions of zinc forms a creamy-white precipitation of zinc nanoparticles. The protein secreted by the microorganisms play as a capping agent, further providing stability to the synthesized nanoparticles [9]. Synthesis of nanoparticles using microorganisms does not involve the use of toxic chemicals; moreover, microbes are easily cultured under laboratory conditions throughout the year, and shows homogeneity in size and shape of obtained nanoparticles [8, 9].

Inflammation is the body's response to harmful stimuli, and cell damage caused by pathogenic invasion results in pain, redness, heat, and swellings. Inflammation-causing cytokines and the generation of reactive oxygen species are primarily accountable for inflammation. The commonly used agent non-steroidal anti-inflammatory drug (NSAID) mainly works by inhibiting prostaglandin. It causes pain and inflammation and has adverse side effects that damage the liver, kidney, gastrointestinal tract, and cardiovascular and renal failure [10]. To alleviate the side effects of NSAID, investigation of natural sources with no toxicity is recommended. Hence, in the present investigation, the anti-inflammatory activity of ZnONPs has been assessed by various methods.

Nanoparticles as a biopesticide have added advantages in crop fields compared to available synthetic pesticides. Zinc oxide nanoparticles (ZnONPs) are semiconductor nanoparticles with wide application in agriculture and related industries. It can degrade the chemical pesticides from the soil by photocatalysis [11]. In recent years, the ZnONPs have even been utilized for their toxicity against major agricultural pests and insects [12]. In most countries, legume cultivation has increased for its valuable products and protein content. Soybean is one such crop with high protein and oil content of commercial importance [13]. In

India, soybean cultivation has been affected by the attack of the green cloverworm (*Hypena scabra*), which damages the plant, ultimately reducing its nutritional value and making it unfit for human consumption [14]. The indiscriminate use of pesticides causes adverse effects on the environment and human health. Hence, researchers are engaged in developing environment-friendly pesticides as a control measure.

With this consideration, current research aims to synthesize *Talaromyces islandicus* mediated ZnONPs, its characterization by various spectroscopic methods, and assessment of antibacterial, anti-inflammatory and pesticidal activity against green cloverworm was conducted.

Materials and Methods

Micro-organism

Talaromyces islandicus VSGF1, a fungal species belonging to the *Trichocomaceae* family, was previously obtained from vermicomposting soil and was used to synthesis ZnONPs. The gene sequence of the fungus was deposited into the Gene Bank database under the accession number MN8186851, and the sub-culture was preserved in NFCCI-ARI, Maharashtra, with deposition no. NFCCI-5020.

Culturing and Preparation of Fungal Filtrate

The *T. islandicus* culture, which had been grown for 24 h, was incorporated into a 100 mL volume of potato dextrose broth (PDB). The PDB was prepared by combining 1000 mL of distilled water with 200 g of potato infusion and 20 g of dextrose at a pH of 6.0 at 27 °C temperature and incubated for 7 days. Subsequently, the culture broth was filtrated using Whatman filter paper No.1, followed by a thorough triple washing with deionized water. A conical flask with a volume of 250 mL was utilized to contain 5 g of fungal mycelium, which was subsequently combined with 100 mL of deionized water. The resulting solution was then subjected to incubation for 24 h. Subsequently, the mycelium underwent filtration, and the resulting filtrate was employed to synthesize ZnONPs.

Synthesis of ZnONPs

A cell-free aqueous fungal filtrate (100 mL) was combined with an equal volume of 0.1 M zinc sulphate ($ZnSO_4.7H_2O$) was added drop wise along with stirring and then heated at 60 °C for 10 min until the formation of white precipitate at the bottom of the flask indicates the formation of zinc oxide nanoparticles (ZnONPs). Then, the nanoparticles were purified by multiple centrifugations at 15,000 rpm for 10 min and the collected pellet was dried at 100 ℃ for further characterization. A limited quantity of sample was collected at 24 and 48 h, and subsequent analysis using UV–Visible spectroscopy was conducted to assess the advancement of particle formation [15, 16].

Characterizations of ZnONPs

The synthesized ZnONPs were characterized through a double-beam UV–Vis. spectroscopic analysis, with measurements taken at a wavelength range of 200 to 700 nm [17]. The functional groups and chemical properties of synthesized nanoparticles through biological processes were explored using Nicolet-6700, a Fourier-transform infrared (FTIR) spectroscopy technique [18]. The FTIR spectrum was acquired within the 4000–450 cm^{-1} wave number range. X-ray diffraction (XRD) is a highly effective method for investigating the characteristics of nanoparticles. The XRD line width, as determined by Debye Scherrer's equation, is frequently employed for particle size measurement. The equation, $d = (0.9\times\lambda) / (\beta\times\cos\theta)$, relates the particle size (d) to the XRD line width, X-ray wavelength (λ), and the angular width of the diffraction peak ($\beta\times\cos\theta$). A scanning electron microscope (SEM) was used to analyze the external frame of ZnONPs and the elemental mapping of zinc oxide NPs. The centrifuged zinc oxide nanoparticles were applied as a coating onto a thin glass film and subsequently analyzed using an SEM analyzer [19]. The involvement of various elementals was identified using equipped energy-dispersive X-ray spectroscopy (EDS) [20]. The Atomic Force Microscopy imaging was conducted using the Nano-surf Easyscan-2 software as described by Daphedar and Taranath [21]. Tapping mode was employed to acquire AFM measurements to gain insights into the surface characteristics.

Antibacterial Activity of ZnONPs

The bacterial test organisms, namely Gram-positive like *Streptococcus pneumoniae* (MTCC 1935), *Enterococcus faecalis* (MTCC 2729), *Staphylococcus epidermidis* (MTCC 6810), and *Staphylococcus aureus* (MTCC 6908) along with Gram-negative such as *Escherichia coli* (MTCC 40), *Pseudomonas aeruginosa* (MTCC 9027), *Salmonella typhi* (MTCC 3224), and *Brevibacillus brevis* (MTCC 7519) were used to perform antibacterial activity by employing agar well diffusion method [22, 23]. The results were documented through measuring the formed zones of inhibition (ZOI) using an antibiotic zone scale. The stock solution of 1 mg/mL ZnONPs was used for the analysis.

Anti-inflammatory Activity

Preparation of HRBC Suspension

The HRBC membrane stabilisation activity was conducted using the methodology outlined by Gandhidasan et al. [24]. The isosaline solution (0.85%) was mixed with a similar volume of whole human blood. A 10 min centrifugation was performed on the sample at a speed of 3000 rpm. The resulting cells were rinsed thrice using isosaline solution (0.85% pH 7.2). The blood volume was quantified and subsequently transformed into a suspension with a concentration of 10% v/v using isosaline.

Heat Induced Haemolysis

The reaction mixture was prepared by combining 2 mL hypo saline [0.36%], 1 mL phosphate buffer [pH 7.4, 0.15 M], 0.5 mL HRBC suspension with 0.5 mL of test samples or standard aspirin at 100 to 500 µg/mL or distilled water (control) were incubated at 37 °C for 30 min and centrifuged, respectively. The haemoglobin concentration was evaluated using a spectrophotometer at 560 nm.

The percentage of haemolysis and stabilization of the HRBC membrane was calculated as follows.

$$\text{Percent Haemolysis} = (\text{Test sample OD}/\text{Control OD}) \times 100.$$

$$\text{Percent Protection} = 100 - \left[(\text{Test sample OD}/\text{Control OD}) \times 100\right].$$

Protein Denaturation Assay

The protocol outlined by Leelaprakash and Dass [25] was utilised in the experiment with a procedure involved combining 1 mL of phosphate-buffered saline (PBS), 50 µL of bovine serum albumin (BSA), and a sample with a concentration ranging from 100 to 250 µg/mL in 1.5 mL of centrifuge tubes. After 15 min of incubation, the mixture was transferred to a hot water bath (70 °C, 15 min) to initiate denaturation. In the experiment, aspirin served as the standard. The absorbance was measured at 660 nm in a UV–Visible spectrophotometer.

The percentage of protein denaturation inhibition was calculated as follows.

$$\text{Percent Protein denaturation activity} = [(\text{control absorbance} - \text{sample absorbance}/\text{control absorbance}] \times 100.$$

Albumin Denaturation Assay

The experimental procedure was conducted in accordance with the protocol outlined by Moharram et al. [26]. In this experiment, a 1 mL of phosphate-buffered saline (PBS), 50 µL of egg albumin, and samples with concentrations ranging from 50 to 250 µg/mL, as well as a standard solution, were combined in 1.5 mL centrifuge tubes and incubated for 15 min at room temperature. Following the incubation period, the tubes were transferred to a hot water bath (70 ℃, 15 min) to initiate the process of denaturation. Aspirin was used as standard in the experiment. The absorbance was measured at 660 nm in UV–Visible spectrophotometer.

The percentage of inhibition of protein denaturation was calculated as follows.

$$\text{Percent Protein denaturation activity} = \left[\text{control absorbance} - \text{sample absorbance}/\text{control absorbance}\right] \times 100.$$

Biopesticidal Activity of ZnONPs

The determination of the lethal concentration of mycosynthesized ZnONPs against the green cloverworm was conducted using the methodology outlined by Kalpana et al. [15]. The control tray was prepared by applying healthy *Glycine max* (Soybean) leaves moistened with water. In the treated tray, the leaves were moistened with a specific concentration of ZnONPs solution (10 mg/100 mL). Approximately 20 healthy green cloverworms were gathered from a field of *Glycine max*. The control and treated trays were each seeded with 10 green cloverworms. These trays were then placed in a room with a consistent temperature, and the worms were allowed to feed on the leaves. The feeding process was observed regularly for 3 days, specifically at 24 h intervals (24, 48, and 72 h). Subsequently, the mortality rate was determined by using the following mathematical formula;

$$\text{Pests mortality}(\%) = \frac{\text{Number of dead larvae}}{\text{Initial number of larvae}} \times 100$$

Study on Seed Germination

The seed germination experiment was performed by adding 10 mg/100 mL of ZnONPs into double distilled water. The *Pisum sativum* seeds of the same size were taken and soaked in the test solution, distilled water (positive control) and $ZnSO_4 \cdot 7H_2O$ (negative control). After 24 h of incubation at room temperature, 10 seeds were transferred to presterilized Petri dishes covered by 2 layers of moistened filter paper at the bottom. The water was sprayed daily to maintain

moisture level and observed seeds for 3 days at 24 h, 48 h and 72 h (Official Seed Analytics (AOSA, 1998). The seed germination was calculated using a formula [27].

Germination percent
= Number of seeds produces normal seedlings/
Number of seeds set for germination × 100

Speed of Germination

Germination Index (GI) was studied standard method (Association of Official Seed Analytical (AOSA, 1983) and the speed of seed germination were calculated by using below formula.

Speed of germination
= Number of seedling/day of first count
+ Number of seedling/day of final count

Root Length, Shoot Length and Seedling Length

On the final day, seedlings were taken, and the length of the roots and shoots were measured from the base to the tip.

Results and Discussion

Visual Observation

The observation of a transition in the colour of the culture filtrate from colourless to the formation of a white precipitate after a 48 h incubation period provides a hint for the synthesis and subsequent deposition of zinc oxide nanoparticles (Fig. 1a). The fungal culture filtrate in the negative control exhibited no observable changes, as depicted in Fig. 1b. The previous study also reported the formation of white precipitate during the synthesis of ZnONPs indicates the production of ZnONPs in solution mixture by using endophytic fungus *Xylaria arbuscula* [9].

Characterization of ZnONPs

UV–Vis Spectroscopy

The reduction of $Zn^{(+2)}$ into $Zn^{(+1)}$ NPs is evidenced by the UV–visible spectral peak of ZnONPs at 298 nm, as depicted in Fig. 2a. The peak observed at approximately 300 nm in the ZnONPs spectrum indicates the occurrence of surface plasmon resonance (SPR). The control solution will not exhibit any discernible peak, as depicted in Fig. 2b. Numerous investigations have been carried

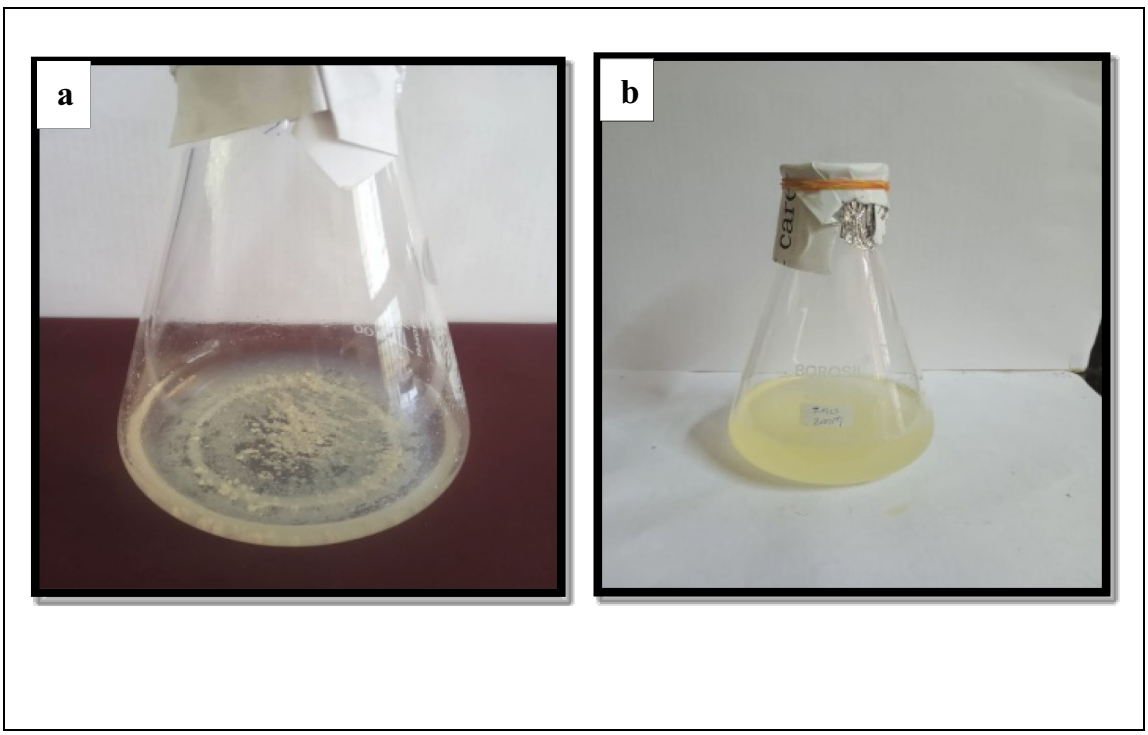

Fig. 1 Visual observation of ZnONPs. **a** Formation of ZnONPs **b** Fungal Culture filtrate

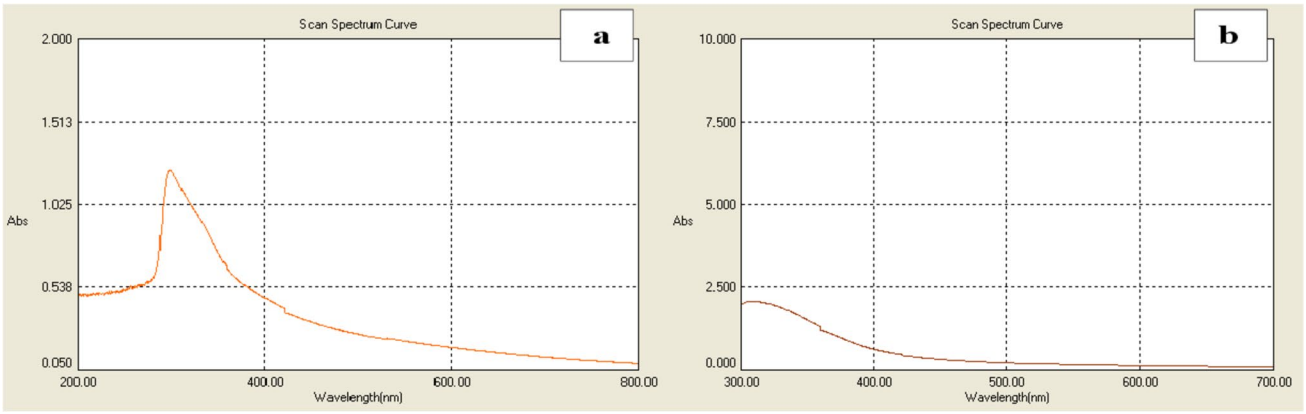

Fig. 2 UV–Visible spectroscopy. **a** Synthesized Zinc oxide nanoparticles, **b** Control sample

out on synthesizing zinc oxide nanoparticles using fungi. These studies have reported absorption peaks at different wavelengths, including 320 to 390 nm [28], 380 nm [29], 350 nm [30], and 380 nm [15], as determined by UV–visible spectrophotometry. These absorption peaks further support the presence of ZnONPs in the culture filtrate.

FT-IR Spectroscopy

The FTIR spectroscopy is used to identify the precise functional groups involved in the production of nanoparticles. The FTIR spectrum of zinc oxide nanoparticles synthesized from *Talaromyces islandicus* exhibited a total of seven discernible peaks at specific wavenumbers, 3457.82, 1690.96, 1438.41, 1164.51, 854.50, 848.36 and 585.00 cm^{-1} (Fig. 3). The spectral peaks recorded in the range of 4000–500 cm^{-1} are attributed to the biotransformation process of metallic zinc oxide nanoparticles. A peak at 3457.82 cm^{-1}, associated with stretching the –OH functional group, indicates the presence of alcohols and phenols. The formation of the amide group occurred at a wavenumber of 1690.96 cm^{-1}. Nitrosamines and –C–O– stretching can be inferred from the peaks observed at 1438.41 and 1164.51 cm^{-1}, respectively. The peak at 1164.51 cm^{-1} also suggests the presence of $–CH_2–$ bending. The presence of a peak at 854.50 cm^{-1} indicates the wagging motion of the $=CH_2$ group, while the formation of a peak at 585.00 cm^{-1} suggests the stretching of the C–Br bond in alkyl halides, as presented in Table 1. According to Baskar et al. [31] identifying these functional groups within zinc oxide nanoparticles contributes to their efficacy as antimicrobial agents. The Fourier-transform infrared (FT-IR) spectra of zinc oxide nanoparticles ZnONPs synthesised by various microorganisms exhibited comparable functional groups, thereby providing additional evidence to corroborate the findings of the current research [15].

XRD Spectrophotometer

The presences of distinct peaks observed in the X-ray diffraction (XRD) spectroscopy at 29, 36, 37, 40, and 45, which correspond to specific crystallographic planes within the face-centred cubic (FCC) structure, demonstrate that the nanoparticles are crystalline. The larger particle size leads to broader and more distinct diffraction peaks. Observing diffraction peaks within the 2θ range of 20° to 80° provides additional evidence supporting the presence of nanoparticles. The nanoparticles (NPs) had an average size of 34 ± 22 nm, as depicted in Fig. 4. The earlier investigation also reported the formation of crystalline nature of nanoparticles with sharp diffraction peak having the size of 41 nm by using *Aspergillus niger* [15].

Atomic Force Microscopy (AFM)

The atomic force microscopy image of ZnONPs synthesised through biological means provides clear evidence of the formation of ZnONPs and their tendency to aggregate, as depicted in Fig. 5. Atomic force microscopy imaging was accomplished through the interaction between the tip and the surface of the sample, thereby enabling the determination of the size and shape of ZnONPs. Visualization of individual or grouped particles, their size, shape and distribution pattern was studied by atomic force microscopy [32]. The analysis validates that the average size range of the synthesised nanoparticles falls within the range of 38 to 52 nm.

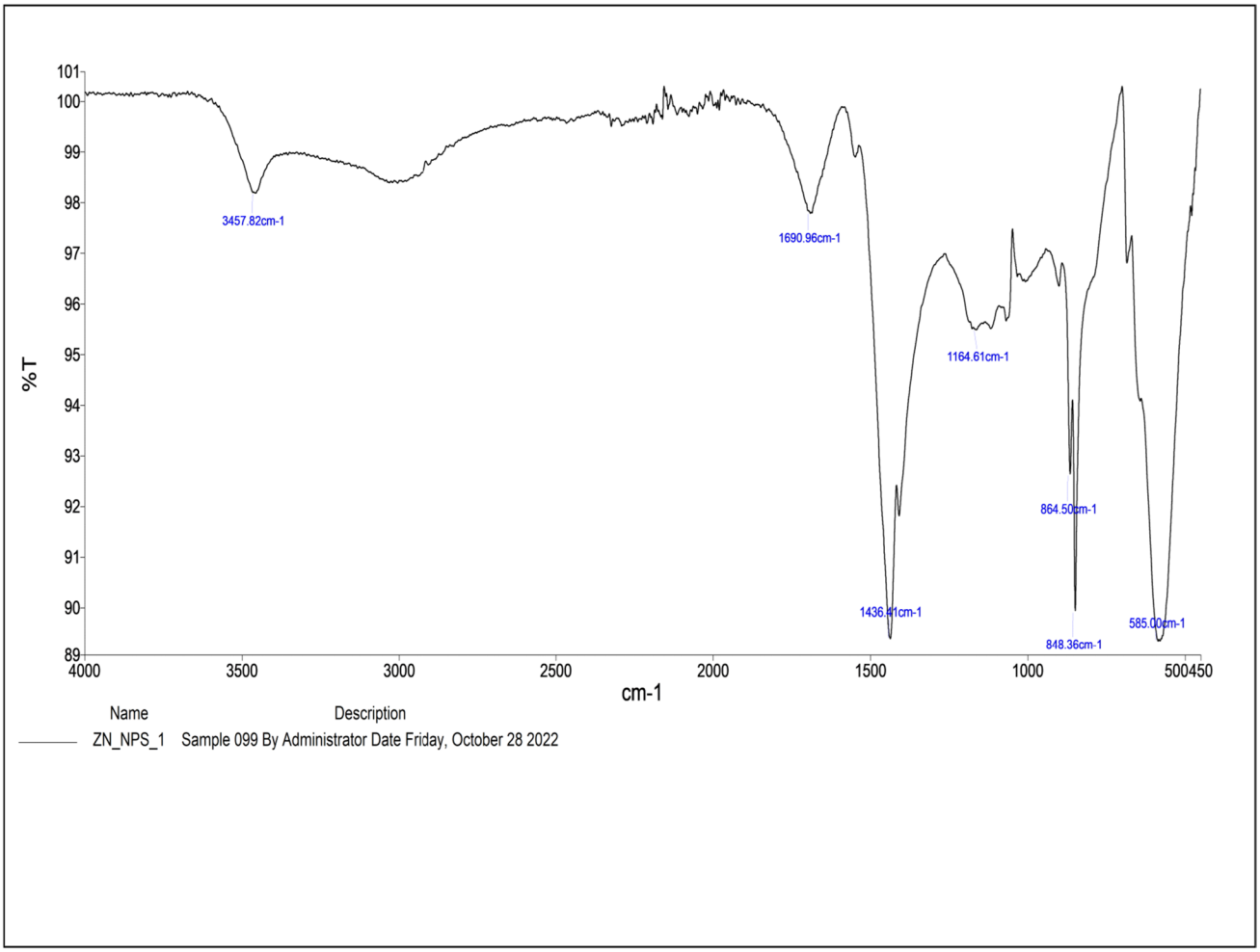

Fig. 3 FT-IR spectrum of synthesized ZnONPs

Table 1 FT-IR absorption peaks and their functional groups of Zinc oxide nanoparticles

Absorption peaks (cm^{-})	Groups involved in NPs synthesis
3457.82	Alcohols and Phenols of –OH stretching
1690.96	Amide C=O group
1438.41	Nitrosamine
1164.51	–C–O– stretching, $–CH_2–$ Bending
854.50	$–CH_2$ Wagging
848.36	–
585.00	Alkyl halides –C–Br-

Scanning Electron Microscopy (SEM)

The nanoparticles of spherical shape and size between 48 to 62 nm were exhibited in SEM images (Fig. 6). By employing Energy Dispersive X-ray spectroscopy at a magnification of 5000×, the formation of zinc oxide nanoparticles was confirmed. The obtained results indicated the presence of a specific combination of elemental components that could be involved in the synthesis of ZnONPs. The spectrum exhibited the most pronounced signals originating from Zinc atoms, while comparatively weaker signals were observed for Oxygen, Sodium, Carbon, and Sulphur particles. The EDX technique records diverse elements by detecting the X-rays emitted from light elements in the K-series and intermediate elements in the L-series (Fig. 7). The study of Raut et al. [33] reported the hexagonal shape of nanoparticles with size ranging 11–25 nm; whereas Emad et al. [34] observed spherical shape of nanoparticles.

Antibacterial Activity of ZnONPs

The antimicrobial efficacy of ZnONPs demonstrated notable antibacterial properties compared to the conventional antibiotic streptomycin. The zone of inhibition measurements of ZnONPs against pathogenic bacteria are presented in Table 2 and Fig. 8. The highest recorded zone of inhibition was 15.33 ± 0.3 mm for *E. faecalis* and 15 ± 0.57 mm

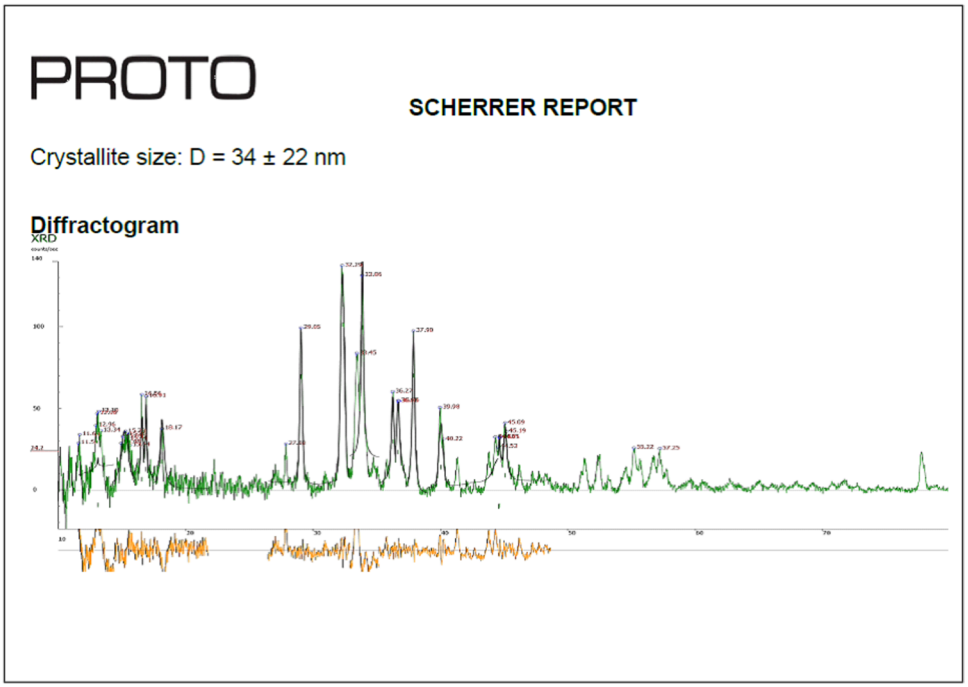

Fig. 4 XRD Scherrer report of synthesized ZnONPs

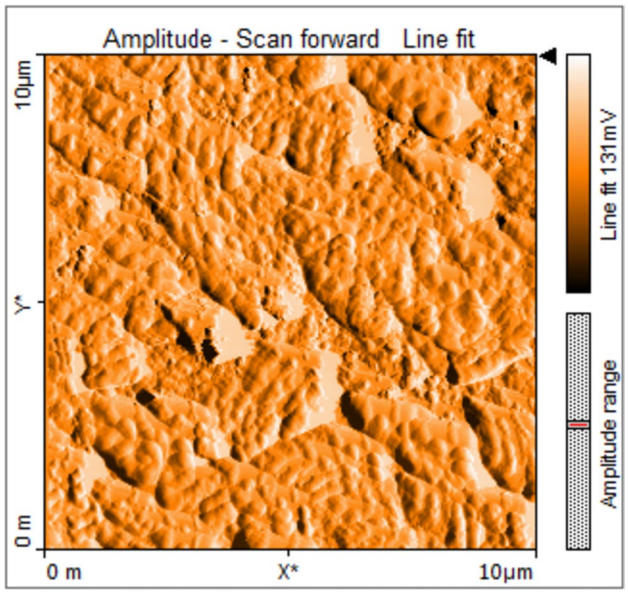

Fig. 5 AFM images of synthesized ZnONPs

for *S. typhi*. Compared to streptomycin, zinc oxide nanoparticles have demonstrated noteworthy efficacy against both *S. aureus* and *S. epidermis*, exhibiting inhibition zones measuring 10.33 ± 0.33 and 13 ± 0.33, respectively. ZnONPs have demonstrated more effectiveness against Gram-positive bacteria than Gram-negative bacteria. Similarly, *Pelargonium odoratissimum*-mediated ZnONPs have antibacterial action against *S. aureus*, *B. cereus*, *P. aeruginosa*, and *E. coli*, with Gram-positive bacteria recording higher inhibition zones than Gram-negative bacteria [35]. Similarly, Stephen and Kennedy [36] examined the effectiveness of synthesised ZnONPs in combating penicillin resistance in *E. coli*. Additionally, Jung et al. [37] investigated the antibacterial properties of these ZnONPs against tobramycin resistance in *P. aeruginosa.*

Anti-inflammatory Activity

HRBC Stabilization Assay

The membrane of human red blood cells (HRBCs) can be compared to the lysosomal membrane. Consequently, a drug that enhances the stability of the erythrocyte membrane may also enhance the stability of the lysosomal membrane. This, in turn, can inhibit the release of lysosomal enzymes and proteases, contributing to cellular inflammation and damage [38]. Therefore, the compound or drug that exhibits membrane stabilisation properties is regarded as an effective candidate for assessing anti-inflammatory activity. The present study utilised ZnONPs (100–500 µg/mL) to evaluate their effects on haemolysis and HRBC membrane stabilisation. The obtained results were subsequently compared to those of standard aspirin. The findings in Table 3 indicate that the HRBC stabilisation of ZnONPs is 74% compared to the standard aspirin, which exhibited a stabilisation rate of 91% at a concentration of 500 µg/mL. This stabilisation effect was observed in a dose-dependent manner against

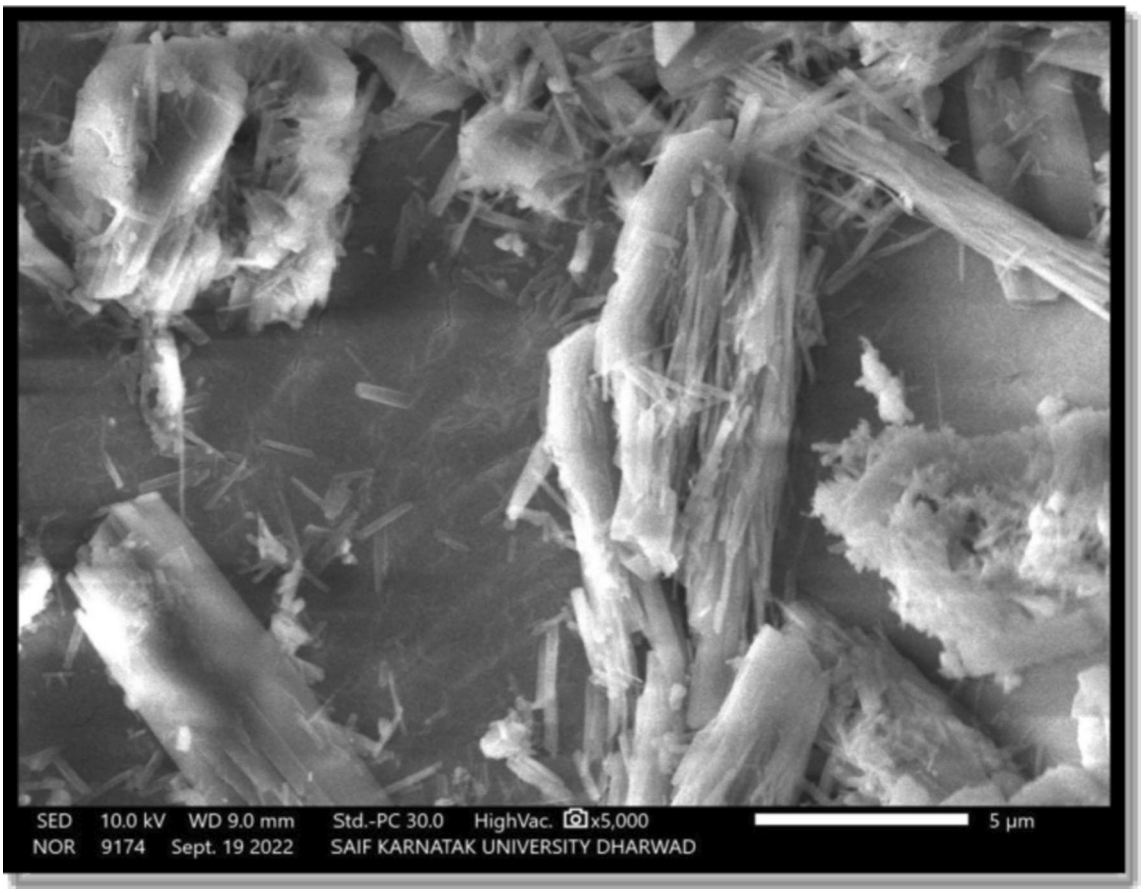

Fig. 6 Scanning electron microscopic image of zinc oxide nanoparticles

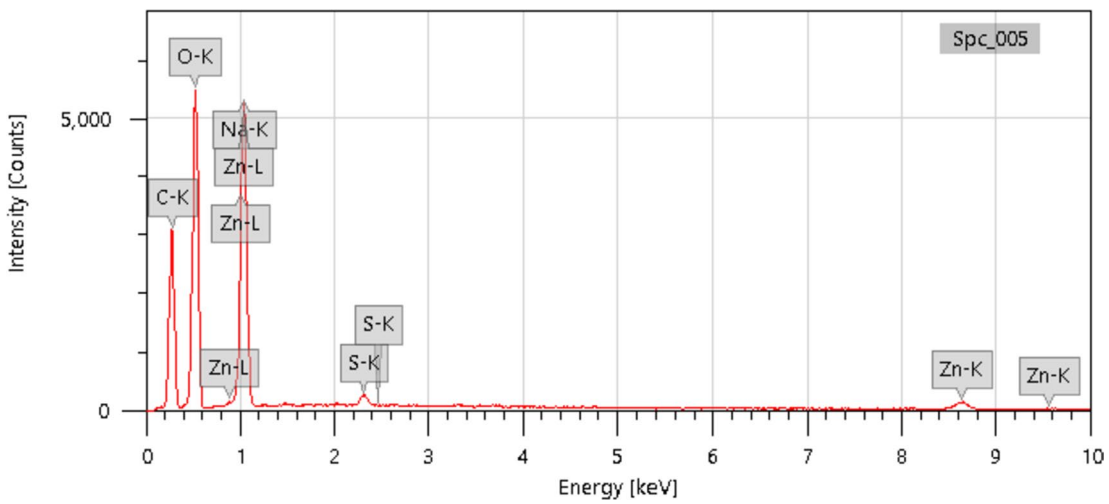

Fig. 7 EDX Spectrum of ZnONPs

Table 2 Antibacterial activity of myco-synthesized ZnONPs

Bacterial strains	Zone of inhibition in mm (mean ± SD)	
	Standard drug Streptomycin	*Talaromyces isalndicus* VSGF-1 ZnONPs
Gram positive		
Enterococcus faecalis	22.33 ± 0.33	15.66 ± 0.33
Staphylococcus aureus	10.67 ± 0.33	10.33 ± 0.33
Streptococcus pneumoniae	12 ± 0.57	13.00
Staphylococcus epidermidis	13.00 ± 0.33	13.00 ± 0.33
Gram negative		
Pseudomonas aeruginosa	10 ± 0.57	8.66 ± 0.33
Escherichia coli	20 ± 0.57	10.66 ± 0.33
Brevibacillus brevis	–	07.33 ± 0.33
Salmonella typhi	20.33 ± 0.33	15 ± 0.57

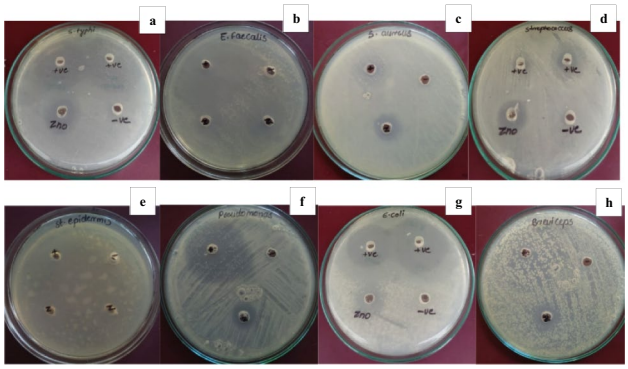

Fig. 8 Antibacterial activity of mycosynthesized ZnONPs. **a** *Salmonella typhi*. **b** *Enterococcus faecalis*. **c** *Staphylococcus aureus*. **d** *Streptococcus sp.* **e** *Staphylococcus epidermidis*. **f** *Pseudomonas aeruginosa*. **g** *Escherichia coli*. **h** *Brevibacillus brevis*

Table 3 Anti-inflammatory activity by HRBC stabilization method

Sample concentrations µg/mL	HRBC % haemolysis Aspirin	ZnONPs	HRBC % stabilization Aspirin	ZnONPs
100	61.3	85.92	38.60	14.07
200	50.90	69.29	49.09	30.70
300	38.18	58.33	61.81	41.66
400	23.64	41.81	76.55	58.18
500	8.98	25.46	91.01	74.53

hypotonicity-induced haemolysis. A hemolysis rate of 25% was observed in ZnONPs at a concentration of 500 µg/mL, while the standard aspirin exhibited a hemolysis rate of 8% at the same concentration. This finding suggests that ZnONPs demonstrate a moderate level of activity.

Table 4 Anti-inflammatory activity by using egg albumin and protein denaturation assay

% anti-inflammatory activity of std. Aspirin and ZnONPs				
Sample Concentrations µg/mL	Egg albumin		Protein denaturation	
Aspirin/ZnONPs	Std	ZnONPs	Std	ZnONPs
50	47.03	28.92	47.48	32.47
100	61.97	37.89	60.67	45.69
150	74.55	48.32	70.20	58.48
200	83.37	58.35	79.52	68.89
250	91.76	73.30	87.47	77.17

BSA and Egg Albumin Protein Denaturation Assay

Protein denaturation is observed within inflamed cells as a response to inflammation, leading to cellular or tissue functionality subsequent impairment. During the denaturation process, proteins are secondary and tertiary structures undergo distortion because of exposure to highly acidic or basic conditions, ultimately resulting in the loss of enzyme activity. An ideal candidate for an anti-inflammatory drug would be an agent that effectively inhibits protein denaturation. Table 4 represents the outcomes of the BSA and egg albumin protein denaturation assay. The present study observed that 250 µg/mL of ZnONPs demonstrated a 77.17% inhibition of BSA protein denaturation and a 73.30% inhibition of egg albumin protein denaturation. These inhibitory effects were found to be of moderate activity when compared to the standard aspirin, which exhibited inhibitions of 87.47 and 91.76% for BSA and egg albumin protein denaturation, respectively. The IC_{50} value of ZnONPs for inhibiting denaturation of BSA protein is 120.94 µg/mL, which is higher than the IC_{50} value of the standard aspirin (53.49 µg/mL). Similarly, the IC_{50} value of ZnONPs for inhibiting denaturation of egg albumin protein is 152.89 µg/mL, also higher than the IC_{50} value of the standard aspirin (51.95 µg/mL). Prior to this, Lopez-Miranda et al. [39] revealed that Sargassum extract-based ZnO nanoparticles had anti-inflammatory activity with an IC_{50} value of 219.13 gmL^{-1} for protein denaturation assay in comparison to standard DFS of 253.73 gmL^{-1}. Similarly, Rajakumar et al. [40] obtained IC_{50}: 222.01 gmL^{-1} using *Andrographis paniculata* induced ZnONPs, while Velsankar et al. [41] reported IC_{50}: 222.01 gmL^{-1} using an *E. variegata* leaf extract.

Biopesticidal Activity of ZnONPs

The biopesticidal potential of various concentrations of myco-synthesized zinc oxide nanoparticles was evaluated against the green cloverworm. The mortality rates

Table 5 Study of biopesticidal activity of ZnONPs

SI. No	Sample	Dose	Percent of pests mortality in days after treatment		
			1	2	3
01	Water	10 mg/10 mL	0	0	0
02	ZnONPs	10 mg/10 mL	28.57%	66.66%	83.33%

observed for the zinc oxide nanoparticles were 28.57, 66.66, and 83.33% at 24, 48, and 72 h, respectively, as presented in Table 5. The larval mortality rate exhibited a positive correlation with both the concentration and duration of treatment. On the initial day, the mortality rate stood at 28.57%; on the third day, it escalated to 83.33%. The mortality rate was directly correlated with the sample quantity to be utilised. A higher level of efficacy was observed with decreasing nanoparticle size. Jameel et al. [42] and Gutiérrez-Ramírez et al. [43] observed comparable findings in their respective studies, reporting a larval mortality rate of 27 and 88% when utilising a composite of ZnONPs with thiamethoxam and ZnONPs alone, respectively. Similarly, according to Thakur et al. [44], increased ZnONPs concentrations increased insect mortality.

Behavioural Changes in Pests After Treatment with Mycosynthesized ZnONPs from *T. islandicus*

Several changes were observed when the exposure of pests to the test concentration of mycosynthesized zinc oxide nanoparticles (ZnONPs) derived from *T. islandicus* (Fig. 9). On the first day, the pest began to lose its colouration. On the third day, the pests transformed, adopting a black colouration and subsequently perishing. The ZnONPs synthesised through mycosynthesis exhibited significant efficacy against the pests, resulting in the cessation of their active movement. Within a 24 h period, the pests' entire bodies became rigid and firm and began to release bodily fluids. Subsequently, the pests exhibited a nearly 'C' shaped form, and within 72 h, they typically displayed signs of premature moulting.

Fig. 9 Pests treated with control sample after **a** 24 h, **b** 48 h, **c** 72 h, and pests treated with ZnONPs After **d** 24 h, **e** 48 h, and **f** 72 h

Jameel et al. [42] also documented comparable outcomes of malformation in pests caused by ZnONPs. According to Pittarate et al. [45], zinc oxide nanoparticles (NPs) have a direct effect on *Spodoptera frugiperda*, where bodily malformations, decreased fecundity, decreased oviposition, and decreased egg hatchability have been reported. The research data shows that the ZnONPs can work as an effective biopesticide, demonstrating their ability to eliminate pests within a relatively brief timeframe.

Effect of ZnONPs on Seed Germination

The impact of mycosynthesized ZnONPs (mg/mL) on seed germination is assessed by measuring germination percentage and speed of germination Table 6 and Fig. 10. The findings indicate that the percentage of seed germination, shot length, and seedling length are more significant in seeds treated with ZnONPs than in the positive control group. The germination and root length rates observed in both the ZnONPs treated group and the positive control group are comparable and significantly greater than those of the negative control group. Prerana et al. [46] showed that ZnO nano-primed seeds have increased seed germination rate and seedling characteristics while working on a maize plant. The other researchers predict that the effect of ZnONPs on seed germination will vary on the dose. While increasing the concentration of ZnONPs after a specific limit will harm the seed germination percentage, applying low concentrations of zinc oxide NPs will enhance germination [47, 48]. While working on a tomato plant, Wodarczyk and Smoliska [49] discovered that the size of ZnONPs also impacted seed germination. They claim that ZnONPs with a 50 nm diameter are better for seeds than NPs with a 100 nm diameter. In contrast, previous studies have documented the phytotoxic impact of ZnONPs on the host plant, resulting in a reduced root length [50, 51]. This study's findings suggest that applying *Talaromyces islandicus* mediated zinc oxide nanoparticles (ZnONPs) to plants can effectively eliminate pests while not negatively impacting seedling growth.

Conclusion

The utilisation of secondary metabolites in the biological approach serves as stabilising and reducing agents, thereby facilitating the formation of nanoparticles with precise

Table 6 Seed germination parameters of mycosynthesized ZnONPs

Sl.No	Sample mg/mL	Germination percentage (%)	Speed of germination	Root length (cm)	Shoot length (cm)	Seedling length (cm)
1	Water (Positive control)	41.7	5.16	2.96	1.21	4.17
2	$ZnSO_4 \cdot 7H_2O$ (Negative control)	39.5	4.83	2.85	1.1	3.95
3	ZnONPs	46	5.16	2.96	1.64	4.6

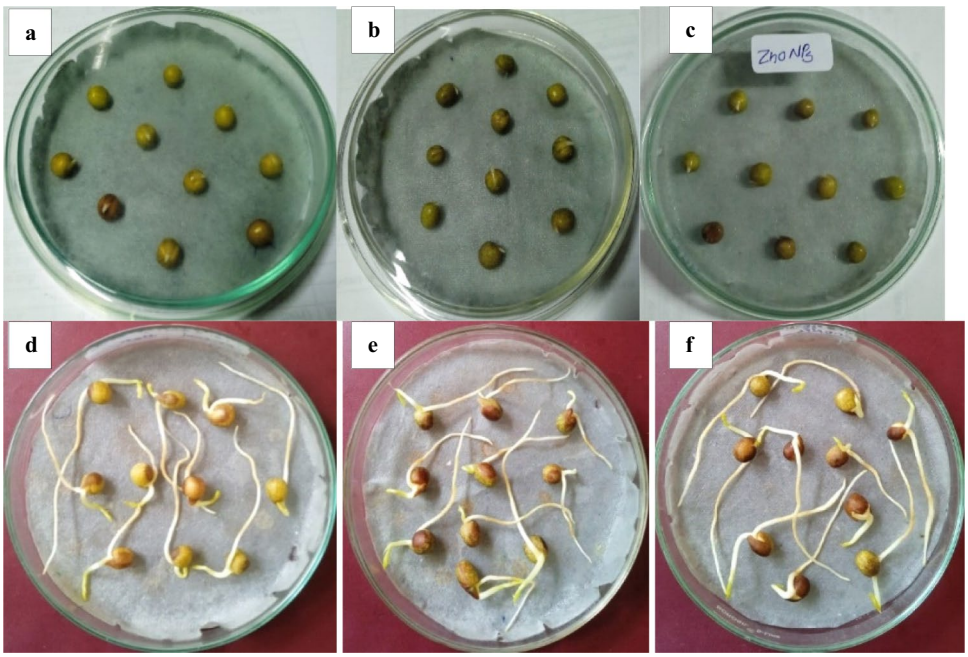

Fig. 10 Seed germination study. Seeds soaking for 24 h. **a** Water. **b** $ZnSO_4$. **c** ZnONPs seed germination after 72 h. **d** Water. **e** $ZnSO_4$. **f** ZnONPs

control over their size and shape. The zinc oxide nanoparticles derived from *T. islandicus* represent a straightforward, cost-effective approach, exhibiting minimal or negligible adverse effects. The synthesised ZnONPs demonstrated efficacy against MDR strains of *E. faecalis* and *S. typhi* at low concentrations. The current research demonstrates that the nanoparticles exhibit noteworthy pesticidal properties against green cloverworm while not causing any detrimental effects on the host plant. The outcome of this study suggests that the ZnONPs derived from *Talaromyces islandicus* hold promise for utilisation in harnessing their biological capabilities. Additional experimentation should be conducted to assess the efficacy of *T. islandicus* mediated ZnONPs against different pathogens, pests, and modes of action. Finally, this study will provide further justification for using this approach.

Author contributions The study conception and design were done by VG. Material preparation, data collection and analysis were performed by MKS, T and PG. The first draft of the manuscript was written by MKS, and review & editing were done by MPB and SKN. Data validation and funding acquisition were done by RSK and SMM. All authors read and approved the final manuscript.

Funding This project was supported by Researchers Supporting Project Number (RSP2024R142), King Saud University, Riyadh, Saudi Arabia.

Data Availability Data will be made available on request.

Declarations

Competing interest The authors have no relevant financial or non-financial interests to disclose.

References

1. Peltonen, L., Hirvonen, J.: Drug nanocrystals—versatile option for formulation of poorly soluble materials. Int. J. Pharm. **537**, 73–83 (2017). https://doi.org/10.1016/j.ijpharm.2017.12.005
2. Moodley, J.S., Krishna, S.B.N., Pillay, K., Sershen, P., G.: Green synthesis of silver nanoparticles from *Moringa oleifera* leaf extracts and its antimicrobial potential. Adv. Nat Sci. **9**, 015011 (2018). https://doi.org/10.1088/2043-6254/aaabb2
3. Zeinab, S., Mojtaba, S., Farad, K.: Biological synthesis of gold nanoparticles by fungus *Epicoccum nigrum*. J. Clus. Sci. **22**, 661–665 (2011)
4. Thangavel, S., Ramasamy, B.: Bio-medically active zinc oxide nanoparticles synthesized by using extremophilic actinobacterium, *Streptomyces* sp. (MA30) and its characterization. Artif. Cells Nanomed. Biotechnol. **45**, 1521–1529 (2017). https://doi.org/10.1080/21691401.2016.1260577
5. Tiwari, V., Mishra, N., Gadani, K., Solanki, P.S., Shah, N.A., Tiwari, M.: Mechanism of anti-bacterial activity of zinc oxide nanoparticle against carbapenem-resistant *Acinetobacter baumannii*. Front. Microbiol. **9**, 1218 (2018). https://doi.org/10.3389/fmicb.2018.01218
6. Gudkov, S.V., Burmistrov, D.E., Serov, D.A., Rebezov, M.B., Semenova, A.A., Lisitsyn, A.B.: A mini review of antibacterial properties of ZnO nanoparticles. Front. Phys. **9**, 641481 (2021). https://doi.org/10.3389/fphy.2021.641481
7. Olechnowicz, J., Tinkov, A., Skalny, A., Suliburska, J.: Zinc status is associated with inflammation, oxidative stress, lipid, and glucose metabolism. J. Physiol. Sci. **68**, 19–31 (2018). https://doi.org/10.1007/s12576-017-0571-7
8. Miri, A., Mahdinejad, N., Ebrahimy, O., Khatami, M., Sarani, M.: Zinc oxide nanoparticles: biosynthesis, characterization, antifungal and cytotoxic activity. Mater. Sci. Eng. **104**, 109981 (2019)
9. Nehru, L., Kandasamy, G.D., Sekar, V., Alshehri, M.A., Panneerselvam, C., Alasmari, A., Kathirvel, P.: Green synthesis of ZnO-Nps using endophytic fungal extract of *Xylaria arbuscula* from *Blumea axillaris* and its biological applications. Artif. Cells Nanomed. Biotechnol. **51**, 318–333 (2023)
10. Mans, D.R.A., Friperson, P., Djotaroeno, M., Misser, S.V., Pawirodihardjo, J.: In vitro anti-inflammatory and antioxidant activities as well as phytochemical content of the fresh stem juice from *Montrichardia arborescens* Schott (Araceae). Pharmacogn. J. **14**, 296–304 (2022)
11. Baruah, S., Dutta, J.: Nanotechnology applications in pollution sensing and degradation in agriculture: a review. Environ. Chem. Let. **7**, 191–204 (2009). https://doi.org/10.1007/s10311-009-0228-8
12. Roni, M., Murugan, K., Panneerselam, C., Suramaniam, J., Nicoletti, M., Madhiyazhagan, P., Dinesh, D., Suresh, U., Khater, H., Wei, H., Canale, A., Alarfaj, A.A., Murgan, A.M., Higuchi, A., Benelli, G.: Characterization and biotoxicity of *Hypnea musciformis*-synthesied silver nanoparticles as potential eco-friendly control tool against *Aedes aegypti* and *Plutella xylostella*. Ecotoxicol. Eniron. Saf. **121**, 31–38 (2015)
13. Wang, J., Zhou, P., Shi, X., Yang, N., Yan, N., Zhao, Q., Yang, C., Guan, Y.: Primary metabolite contents are correlated with seed protein and oil traits in near-isogenic lines of soybean. The Crop J. **7**, 651–659 (2019). https://doi.org/10.1016/j.cj.2019.04.002
14. Christensen, C.M., Kaufmann, H.H.: Deterioration of stored grains by fungi. Ann. Rev. Phytopathol. **3**, 69–84 (2003)
15. Kalpana, V.N., Kataru, B.A.S., Sravani, N., Vigneshwari, T., Panneeresevam, A., Devi Rajeswari, V.: Biosynthesis of zinc oxide nanoparticle using culture filtrate of *Aspergillus niger*: antimicrobial textiles and dye degradation studies. OpenNano. **3**, 40–55 (2018)
16. Jain, D., Shivani, B., A., Singh, H., Daima, H.K., Singh, M., Mohanty, S.R., Stephen, B.J., Singh, A.: Microbial fabrication of zinc oxide nanoparticles and evaluation of their antimicrobial and photocatalytic properties. Front. Chem. **8**, 778 (2020). https://doi.org/10.3389/fchem.2020.00778
17. Chakraborty, B., Bhat, M.P., Basavarajappa, D.S., Rudrappa, M., Nayaka, S., Kumar, R.S., Almansour, A.I., Perumal, K.: Biosynthesis and characterization of polysaccharide-capped silver nanoparticles from *Acalypha indica* L. and evaluation of their biological activities. Env. Res. **225**, 115614 (2023)
18. Pallavi, S.S., Bhat, M.P., Nayaka, S.: Microbial synthesis of silver nanoparticles using *Streptomyces* sp. PG12 and their characterization, antimicrobial activity and cytotoxicity assessment against human lung (A549) and breast (MCF-7) cancer cell lines. Int J Pharm Pharm Sci **13**, 94–102 (2021)
19. Shashiraj, K.N., Nayaka, S., Kumar, R.S., Kantli, G.B., Basavarajappa, D.S., Gunagambhire, P.V., Almansour, A.I., Perumal, K.: *Rotheca serrata* flower bud extract mediated bio-friendly preparation of silver nanoparticles: their characterizations, anticancer, and apoptosis inducing ability against pancreatic ductal adenocarcinoma cell line. Processes **11**, 893 (2023)
20. Shashiraj, K.N., Hugar, A., Kumar, R.S., Rudrappa, M., Bhat, M.P., Almansour, A.I., Perumal, K., Nayaka, S.: Exploring the

antimicrobial, anticancer, and apoptosis inducing ability of biofabricated silver nanoparticles using *Lagerstroemia speciosa* flower buds against the human osteosarcoma (MG-63) cell line via flow cytometry. Bioeng. **10**, 821 (2023)
21. Daphedar, A., Taranath, T.C.: Characterization and cytotoxic effect of biogenic silver nanoparticles on mitotic chromosomes of *Drimia polyantha* (Blatt. and McCann) Stearn. Toxicol. Rep. **5**, 910–918 (2018)
22. Magaldi, S., Mata-Essayag, S., Hartung, C.C., Perez, C., Colella, M.T., Olaizola, Y.O.: Well diffusion for antifungal susceptibility testing. Int. J. Infect. Dis. **8**, 39–45 (2016)
23. Math, H.H., Shashiraj, K.N., Kumar, R.S., Rudrappa, M., Bhat, M.P., Basavarajappa, D.S., Almansour, A.I., Perumal, K., Nayaka, S.: Investigation of in vitro anticancer and apoptotic potential of biofabricated silver nanoparticles from *Cardamine hirsuta* (L.) leaf extract against Caco-2 cell line. Inorg. **11**, 322 (2023)
24. Gandhidasan, R., Thamaraichelvan, A., Baburaj, S.: Anti- inflammatory action of *Lannea coromandelica* by HRBC membrane stabilization. Fitoterapia **12**, 1–83 (1991)
25. Leelaprakash, G., Dass, S.M.: Invitro anti-inflammatory activity of methanol extract of *Enicostemma axillare*. Int. J. Drug Dev. Res. **3**, 189–196 (2011)
26. Moharram, A., Omar, A., El-Ghani, H.: In vitro assessment of antimicrobial and anti-inflammatory potential of endophytic fungal metabolites extracts. Eur. J. Biol. Res. **7**, 234–244 (2017). https://doi.org/10.5281/zenodo.839696
27. Meher, B.B., Sahu, S., Singhal, S., Joshi, M., Maan, P., Gautam, S.: Influence of green synthesied zinc oxide nanoparticles on seed germination and seedling growth in wheat (*Triticum aestium*). Int. J. Curr. Microbiol. App. Sci. **9**, 258–270 (2020)
28. Jamdagni, P., Khatri, P.J.S., Rana, J.: Green synthesis of zinc oxide nanoparticles using flower extract of *Nyctanthes arbortristis* and their antifungal activity. King Saud Uni. Sci. **30**, 168–175 (2018)
29. Santhoshkumar, J., Kumar, V.S., Rajeshkumar, S.: Synthesis zinc oxide nanoparticles using plant leaf extract against urinary tract infection pathogen. Resour.-Effic. Technol. **3**, 459–465 (2017)
30. Sangeetha, G., Rajeshwari, S., Venkatesh, R.: Green synthesized Zno nanoparticles against bacterial and fungal pathogens. Int. J. Prog. Nat. Sci. Mater. **22**, 693–700 (2012)
31. Baskar, G., Chandhuru, J., Fahad, S.K., Praeven, A.S.: Mycological synthesis characterization and antifungal activity of zinc oxide nanoparticles. Asian J. Pharm. Tech. **3**, 142–146 (2013)
32. Rao, A., Schoeneberger, M., Gnecco, E., Glaezel, T., Meyer, E., Brandlin, D., Scandella, L.: Characterization of nanoparticles using atomic force microscopy. J. Phys. **61**, 971–976 (2007)
33. Raut, S., Thorat, P.V., Thakre, R.: Green synthesis of zinc oxide (ZnO) nanoparticles using *Ocimum tenuiflorum* leaves. Int. J. Sci. Res. **4**, 1225–1228 (2015)
34. Emad, J.I., Karkaz, M.T., Mahmood, K.S., Amin, S.B.: Biosynthesis of zinc oxide nanoparticles and assay of antibacterial activity. Am. J. Biochem. Biotechnol. **13**, 63–68 (2017)
35. Abdelbaky, A.S., Abd El-Mageed, T.A., Babalghith, A.O., Selim, S., Mohamed, A.M.H.A.: Green synthesis and characterization of ZnO nanoparticles using *Pelargonium odoratissimum* (L.) aqueous leaf extract and their antioxidant, antibacterial and anti-inflammatory activities. Antioxidants **11**, 1444 (2022). https://doi.org/10.3390/antiox11081444
36. Stephen, T.O., Kennedy, K.A.: Prevalence of multidrug-resistant *Escherichia coli* isolated from drinking water sources. Int. J. Microbiol. (2018). https://doi.org/10.1155/2018/7204013
37. Jung, R., Fish, D.N., Obritsch, M.D., Maclaren, R.: Surveillance of multidrug resistant *Pseudomonas aeroginosa* in an urban tertiary-care teaching hospital. J. Hosp. Infect. **57**, 105–111 (2004). https://doi.org/10.1016/j.jhin.2004.03.001
38. Yesmin, S., Paul, A., Naz, T., Rahman, A.B.M., Akhter, S.F., Wahed, M.I., Emran, T.B., Siddiqui, S.A.: Membrane stabilization as a mechanism of the anti-inflammatory activity of ethanolic root extract of Choi (*Piper chaba*). Clin. Phytosci. **6**, 59 (2020). https://doi.org/10.1186/s40816-020-00207-7
39. Lopez-Miranda, J.L., Molina, G.A., González-Reyna, M.A., España-Sánchez, B.L., Esparza, R., Silva, R., Estévez, M.: Antibacterial and anti-inflammatory properties of ZnO nanoparticles synthesized by a green method using *Sargassum* extracts. Int. J. Mol. Sci. **24**, 1474 (2023). https://doi.org/10.3390/ijms24021474
40. Rajakumar, G., Thiruvengadam, M., Mydhili, G., Gomathi, T., Chung, I.M.: Green approach for synthesis of zinc oxide nanoparticles from *Andrographis paniculata* leaf extract and evaluation of their antioxidant, anti-diabetic, and anti-inflammatory activities. Bioprocess Biosyst. Eng. **41**, 21–30 (2017). https://doi.org/10.1007/s00449-017-1840-9
41. Velsankar, K., Venkatesan, A., Muthumari, P., Suganya, S., Mohandoss, S., Sudhahar, S.: Green inspired synthesis of ZnO nanoparticles and its characterizations with biofilm, antioxidant, anti-inflammatory, and anti-diabetic activities. J. Mol. Struct. **1255**, 132420 (2022). https://doi.org/10.1016/j.molstruc.2022.132420
42. Jameel, M., Shoeb, M., Khan, M.T., Ullah, R., Mobin, M., Farooqi, M.K., Adnan, S.M.: Enhanced insecticidal activity of thiamethoxam by zinc oxide nanoparticles: a novel nanotechnology approach for pest control. ACS Omega **5**, 1607–1615 (2020)
43. Gutiérrez-Ramírez, J.A., Betancourt-Galindo, R., Aguirre-Uribe, L.A., Cerna-Chávez, E., Sandoval-Rangel, A., Ángel, E.C., Chacón-Hernández, J.C., García-López, J.I., Hernández-Juárez, A.: Insecticidal effect of zinc oxide and titanium dioxide nanoparticles against *Bactericera cockerelli* Sulc. (Hemiptera: Triozidae) on tomato *Solanum lycopersicum*. Agronomy **11**, 1460 (2021). https://doi.org/10.3390/agronomy11081460
44. Thakur, P., Thakur, S., Kumari, P., Shandilya, M., Sharma, S., Poczai, P., Alarfaj, A.A., Sayyed, R.Z.: Nano-insecticide: synthesis, characterization, and evaluation of insecticidal activity of ZnO NPs against *Spodoptera litura* and *Macrosiphum euphorbiae*. Appl. Nanosci. **12**, 3835–3850 (2022). https://doi.org/10.1007/s13204-022-02530-6
45. Pittarate, S., Rajula, J., Rahman, A., Vivekanandhan, P., Thungrabeab, M., Mekchay, S., Krutmuang, P.: Insecticidal effect of zinc oxide nanoparticles against *Spodoptera frugiperda* under laboratory conditions. Insects **12**, 1017 (2021). https://doi.org/10.3390/insects12111017
46. Itroutwar, P.D., Kasivelu, G., Raguraman, V., Malaichamy, K., Sevathapandian, S.K.: Effects of biogenic zinc oxide nanoparticles on seed germination and seedling vigor of maize (*Zea mays*). Biocatal. Agric. Biotechnol. **29**, 101778 (2020). https://doi.org/10.1016/j.bcab.2020.101778
47. Khanm, H., Vaishnavi, B.A., Shankar, A.G.: Raise of nano-fertilizer era: effect of nano scale zinc oxide particles on the germination, growth and yield of tomato (*Solanum lycopersicum*). Int. J. Curr. Microbiol. Appl. Sci. **7**, 1861–1871 (2018). https://doi.org/10.20546/ijcmas.2018.705.219
48. Sarkhosh, S., Kahrizi, D., Darvishi, E., Tourang, M., Haghighi-Mood, S., Vahedi, P., Ercisli, S.: Effect of zinc oxide nanoparticles (ZnO-NPs) on seed germination characteristics in two Brassicaceae family species: *Camelina sativa* and *Brassica napus* L. J. Nanomater. (2022). https://doi.org/10.1155/2022/1892759
49. Włodarczyk, K., Smolińska, B.: The effect of nano-ZnO on seeds germination parameters of different tomatoes (*Solanum lycopersicum* L.) cultivars. Molecules **27**, 4963 (2022). https://doi.org/10.3390/molecules27154963

50. García-López, J.I., Zavala-García, F., Olivares-Sáenz, E., Lira-Saldívar, R.H., Barriga-Castro, D.E., Ruiz-Torres, N.A., Cortez, R.E., Vázquez-Alvarado, R., Niño-Medina, G.: Zinc oxide nanoparticles boosts phenolic compounds and antioxidant activity of *Capsicum annuum* L. during germination. Agronomy **8**, 215 (2018)
51. Burman, U., Saini, M., Kumar, P.: Effect of zinc oxide nanoparticles on growth and antioxidant system of garckpea seedlings. Toxicol. Environ. Chem. **95**, 605–612 (2013)

Authors and Affiliations

M. K. Sangeeta[1] · Tejashree[1] · Vidyasagar M. Gunagambhire[1] · Meghashyama Prabhakara Bhat[2] · Shashiraj Kariyellappa Nagaraja[2] · Pooja V. Gunagambhire[2] · Raju Suresh Kumar[3] · Sakkarapalayam M. Mahalingam[4]

✉ Vidyasagar M. Gunagambhire
gmvidyasagar@gmail.com

[1] Present Address: Department of Botany, Gulbarga University, Kalaburagi, Karnataka 585106, India

[2] Present Address: Department of Studies in Botany, Karnatak University, Dharwad, Karnataka 580003, India

[3] Present Address: Department of Chemistry, College of Science, King Saud University, P.O. Box. 2455, Riyadh, 11451, Saudi Arabia

[4] Present Address: Department of Chemistry, Purdue University, 720 Clinic Drive, West Lafayette, IN 47907, USA